

Gap Properties of Semiconductor Alloys

R. B. Capaz* and Belita Koiller

*Departamento de Física, Pontifícia Universidade Católica do Rio de Janeiro
Cx Postal 38071, 22452 Rio de Janeiro, RJ, Brasil*

Received December 14, 1992; revised manuscript received March 16, 1993

Features of experimental interest in $\text{Al}_x\text{Ga}_{1-x}\text{As}$ and $\text{In}_x\text{Ga}_{1-x}\text{P}$ alloys are studied through a new theoretical treatment, based on the *small crystal* approach. Different alloy configurations accommodated in a relatively large basic cluster are numerically generated and solved independently. Periodic boundary conditions are imposed. The alloy's properties are identified to an *ensemble* average over those calculated for a large number of *small crystal* configurations generated according to the overall composition and degree of order. For randomly disordered $\text{Al}_x\text{Ga}_{1-x}\text{As}$, we focus on the direct-to-indirect transition in the nature of the optical gap, which occurs at $x_c \simeq 0.4$. Physical aspects of the transition are discussed and explored in analogy with order-disorder transitions in statistical mechanics. For $\text{In}_x\text{Ga}_{1-x}\text{P}$, ordering into the experimentally observed monolayer superstructure along the $[111]$ direction is considered. The band-gap energy and structural properties of partially ordered alloys are determined. The dependence of the calculated properties on the long-range order parameter is found to follow simple functional relationships. Structural anisotropies scale accurately with the square of the order parameter. Our results are in good quantitative agreement with the experimentally reported order-induced band-gap narrowing effect.

I. Introduction

$\text{Al}_x\text{Ga}_{1-x}\text{As}$ alloys have been extensively studied during the last years due to their primary importance in high-speed electronic and optoelectronic devices. This development was only possible because these alloys exhibit distinct electronic properties as the composition is changed, but are essentially lattice matched over the whole composition range. The artificial growth of different kinds of structures with controlled electronic and optical properties is thus facilitated. Optimized use of these materials must be based on accurate knowledge of the alloy's properties as a function of composition. Particularly relevant characteristics in this respect are related to the band gap and its optical nature. GaAs is a direct-gap material, while the main energy gap of AlAs is indirect. Therefore, as observed experimentally^[1], progressive substitution of Ga by Al must change the nature of the gap in the alloy towards an indirect-gap behavior. Usual theoretical pictures describing the direct-to-indirect gap transition in $\text{Al}_x\text{Ga}_{1-x}\text{As}$ are based on interpolation schemes connecting the band structures of the binary constituents. The top of the valence band is expected to remain of Γ symmetry for all x , while a Γ - X conduction-band-edge crossover is presumed to occur at a transition composition x_c , above which the gap becomes indirect^[1,2]. This is strictly not the case, since alloys are not translation-

ally invariant, and therefore \vec{k} is not a good quantum number except for $x = 0$ or 1 . This crossover must be understood within a theory which does not rely on zinc-blende symmetry points in reciprocal space, and which allows for z_2 and other properties related to the transition to be calculated.

$\text{In}_x\text{Ga}_{1-x}\text{P}$ alloys are also very convenient light emitting materials for device applications, due to their large direct band-gap and to a close lattice match to GaAs at $x = 0.5$. Special attention has been given lately to the experimental observation of spontaneous ordering of this alloy into a metastable structure, and to the consequences of this ordering in the electronic properties of the material, particularly the order-induced band-gap narrowing. Relative to the random alloy at $x = 0.5$, a band-gap narrowing of over 100 meV has been observed in ordered samples^[3-5]. Accurate determination of the long-range order (LRO) parameter is essential in the investigation of the mechanisms leading to ordering as well as to establish the effect of different growth parameters in ordering^[6].

Conventional alloy approximations are inadequate for the theoretical treatment of the problems mentioned above. Such techniques^[2] usually involve approximating the system's Hamiltonian or Green's function by an effective operator representing the corresponding configurational average over the alloy, and from which alloy's properties are obtained. The averaging procedure casts the problem into a higher-symmetry environment, which for $\text{A}^{\text{III}}\text{B}^{\text{III}}\text{C}^{\text{V}}$ semiconductor alloys is commonly

*Present address: Department of Physics, Massachusetts Institute of Technology, Cambridge, MA 02139.

taken to be zinc-blende. The wave-function symmetry is accordingly constrained, and therefore a poor or incomplete description results for related properties, such as the nature of the gap in $\text{Al}_x\text{Ga}_{1-x}\text{As}$. Also, full or partial ordering of $\text{In}_x\text{Ga}_{1-x}\text{P}$ can not be mapped into a zinc-blende symmetry problem, since the primitive cell for the observed ordered structure does not fit into the zinc-blende primitive cell.

We treat disordered alloys in the small crystal approach^[7-9], and show that the difficulties mentioned above are properly handled in this context. Specific alloy properties are identified to configurational averages of these properties calculated for the ordered compounds accommodated within a given basic cluster. The accuracy of this assumption increases with the basic cluster size, becoming exact in the limit of an infinite cluster. In order to simulate an infinite solid, periodic boundary conditions are imposed. Occupational correlations within the basic cluster size are preserved. In Section II we discuss the crossover in the optical nature of the gap of $\text{Al}_x\text{Ga}_{1-x}\text{As}$ alloys. Results for the electric dipole moment associated to the main gap transition, obtained with basic cluster sizes ranging from 16 to 216, are presented and compared to the virtual crystal approximation results. Structural properties and the energy gap of partially ordered $\text{In}_x\text{Ga}_{1-x}\text{P}$ alloys are considered in Section III, where we discuss the possibility of inferring the order parameter from measurements of these properties.

II. Direct-to-Indirect gap transition in $\text{Al}_x\text{Ga}_{1-x}\text{As}$

The small crystal approach^[10] is equivalent, for ordered systems, to a sampling over a small number of points in the Brillouin zone of the infinite, periodic lattice. A basic cluster of sites is chosen, and different configurations are defined according to their specific occupation, with periodic boundary conditions imposed. For a 16-site basic cluster in the diamond lattice, the inequivalent structures for $\text{A}_n^{\text{III}}\text{B}_{8-n}^{\text{III}}\text{C}_8^{\text{V}}$ compounds are systematically classified in Ref. [7]. Disordered $\text{A}_x^{\text{III}}\text{B}_{1-x}^{\text{III}}\text{C}^{\text{V}}$ alloy's properties are approximated by configurational averages over the ordered structures accommodated in a given cluster size. Averages may thus be exactly performed for a 16-site cluster, namely

$$P(x) = \frac{\sum_{S_\xi} x^n (1-x)^{8-n} D(S_\xi) P(S_\xi)}{\sum_{S_\xi} x^n (1-x)^{8-n} D(S_\xi)}, \quad (1)$$

where \mathbf{P} is any alloy property and $P(S_\xi)$ is the value of this property calculated for the ordered compound structure S_ξ . The sums are performed over the inequivalent structures $\{S_\xi\}$, $D(S_\xi)$ is the degeneracy of configuration S_ξ , and n is the number of A^{III} atoms in the basic cluster for this configuration.

Improved alloy approximations are obtained by increasing the basic cluster size C . However, the number of possible configurations increases exponentially with C , and a systematic classification of the inequivalent ones becomes impractical as the basic cluster size increases. For example, changing C from 16 to 64 leads to a factor of over 7 orders of magnitude increase in the number of possible configurations. This difficulty is overcome by the standard statistical procedure of replacing the configurational average by an ensemble average performed over a representative set of structures generated numerically according to the occupation probabilities of the sites of the group-III sublattice. For a random $\text{Al}_x\text{Ga}_{1-x}\text{As}$ alloy, these are $p_{\text{Al}} = x$ and $p_{\text{Ga}} = 1 - x$. Random $\text{Al}_x\text{Ga}_{1-x}\text{As}$ is thus simulated by a number N of small crystal structures $\{S_\ell\}$, whose basic cluster configurations provide a realistic sampling of C -atom cells extracted from the macroscopic system.

We describe electronic properties of $\text{Al}_n\text{Ga}_m\text{As}_{m+n}$ ordered compounds within the tight-binding formalism, with Hamiltonian matrix elements taken from the parametrization suggested by Vogl *et al.*^[11] for the binary constituents GaAs and AlAs. Such parametrization reproduces the major features of conduction and valence bands of these compounds. The basis set is of type sp^3s^* , where s^* refers to an excited effective s orbital, and the Hamiltonian for each small crystal configuration is obtained according to the sites occupation. In order to account for the valence band-edge discontinuity, the on-site elements of AlAs are shifted downward with respect to those for GaAs by 0.47 eV. Environmental disorder at the group-V sublattice is dealt with by taking for the on-site As matrix elements the average of the parameters for As in the binary compounds weighted by the number of Ga and As atoms among its four neighbors.

The nature of the gap of a compound with structure S_ℓ is related to the electric dipole moment, $\vec{M}(S_\ell) = \langle v_\ell | \vec{p} | c_\ell \rangle$, which vanishes for indirect-gap materials. The transition matrix element above is related to the states $|c_\ell\rangle$, at the bottom of the conduction band, and $|v_\ell\rangle$, at the top of the valence band. This quantity is easily calculated in the tight-binding approach, since in the basis set $\{|i, \mu\rangle\}$, with i representing the site and μ representing the orbital^[8],

$$\langle i, \mu | \vec{p} | j, \nu \rangle \simeq \frac{im}{\hbar} \langle i, \mu | H | j, \nu \rangle \vec{r}_{ij}. \quad (2)$$

The dipole moment $\vec{M}(S_\ell)$ is thus obtained from the Hamiltonian matrix elements and from the eigenfunctions calculated in the tight-binding basis set. Within the small crystal treatment, $M^2(x)$ for an $\text{Al}_x\text{Ga}_{1-x}\text{As}$ alloy is approximated by the ensemble average of $|\vec{M}(S_\ell)|^2$, with $\text{Al}_n\text{Ga}_m\text{As}_{m+n}$ structures S_ℓ defined in a $C = 2(n+m)$ -site basic-cluster.

In Fig 1 we present results for $M^2(x)$ calculated for basic cluster sizes $C = 16, 64$ and 216. Note that

for $C = 16$, M^2 is a smoothly decreasing function of x , with no indication of a crossover from direct-to-indirect gap regimes^[8]. Results for this basic cluster size are obtained from exact configurational averages, as indicated in Eq.(1). For $C = 64$, ensembles with $N = 400$ configurations were generated for each value of x . Statistical error bars are given for the data points (triangles). An indirect-gap region is identified above $x \simeq 0.4$. The direct-to-indirect gap crossover is even clearer from the $C = 216$ results (squares), calculated from $N = 40$ configurations for each value of x . The indirect-gap region appears above $x \simeq 0.5$, while a sharp decrease in M^2 occurs in the composition range from 0.35 to 0.45. Results for $M^2(x)$ calculated within the virtual crystal approximation (VCA) are also presented. Matrix elements are linearly interpolated from the binary constituents, and a zinc-blende symmetry Hamiltonian results for the whole composition range. The calculated M^2 presents a negligible decrease with x (less than 1%) as x increases from 0 to 0.3, where it drops discontinuously to zero. At the composition $x_c^{VCA} = 0.3$, a conduction-band-crossing occurs, leading to a strictly indirect-gap situation for $x > x_c^{VCA}$.

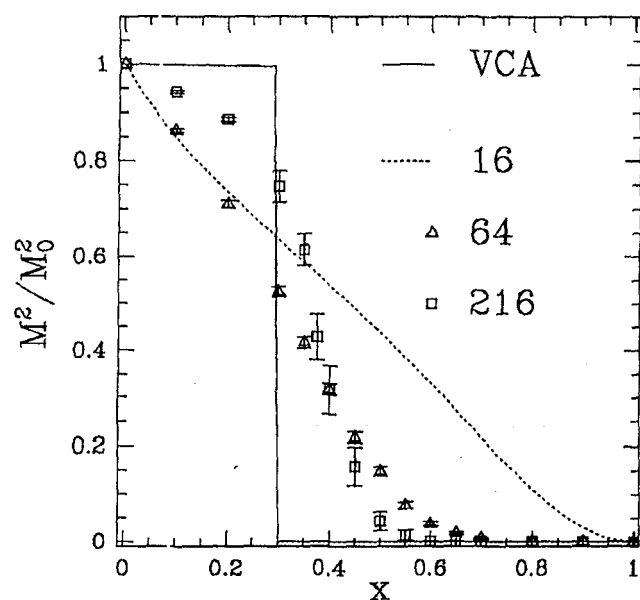


Figure 1: Dipole moment squared for the main gap transition of $\text{Al}_x\text{Ga}_{1-x}\text{As}$, normalized to the GaAs value, vs alloy composition x . Calculations within the small crystal approximation and basic cluster sizes $C = 16, 64$ and 216 are given by the dotted line, triangles and squares respectively. The solid line is the result obtained in the virtual crystal approximation.

Comparison of the results for different levels of the small crystal approximation show a tendency towards sharper direct-to-indirect gap transitions as the basic cluster size C increases. At the transition region, larger

statistical error bars are obtained, another indication that for $C \rightarrow \infty$, a well defined critical concentration x_c may be found at which M^2 goes to zero. From the present results, a value of x_c between 0.4 and 0.5 is to be expected, which is in good agreement with experiments^[1]. The analytic behavior of the transition is hard to be inferred from the present results. Note that this problem may be studied in analogy with order-disorder transitions in statistical mechanics, where M^2 naturally defines the associated order parameter. Formally, it is important to establish whether the order parameter goes continually (second order transition) or discontinuously (first order transition) to zero. Effective-potential approximations lead to first order transitions, as illustrated by the VCA calculations in Fig 1. However, this result is implied by the underlying approximations and by the related band-crossing picture criterion for the transition. The small crystal approach provides, for increasing values of C , a hierarchy of approximations for alloy properties from which infinite-system values may be extrapolated through Monte Carlo statistical mechanics techniques^[12,13]. Calculations under way, for larger values of C and aiming at these questions, shall be reported elsewhere.

III. Structural and gap properties of partially ordered $\text{In}_{0.5}\text{Ga}_{0.5}\text{P}$

The band-gap energy (E_g) of $\text{In}_{0.5}\text{Ga}_{0.5}\text{P}$ alloys grown on (001) GaAs substrates by metalorganic vapor phase epitaxy^[3-6,14] and atomic layer epitaxy^[15] is found to depend strongly on the growth conditions. According to the growth parameters, values for E_g ranging from 1.78 eV to 1.92 eV at 300 K^[3,4,15] and from 1.882 eV to 1.987 eV at 13 K^[5] have been measured. Gomyo *et al.*^[3,4] qualitatively related this gap narrowing to the degree of ordering in the alloy's group-III sublattice. Samples producing stronger superstructure spots in the electron-diffraction patterns also presented narrower gaps^[4]. Kanata *et al.*^[5] assumed that E_g decreases linearly with the LRO parameter in these alloys. On the other hand, Kurtz *et al.*^[16] pointed out that the correlation between the degree of long-range order (LRO) in $\text{In}_{0.5}\text{Ga}_{0.5}\text{P}$ and changes in the band gap properties is not yet established in detail. They find samples with almost "normal" band gaps but still showing a significant degree of order in X-ray diffraction patterns.

The observed ordered structure is the $(\text{GaP})_1/\text{InP}_1$ monolayer superstructure along the $[111]$ direction. We define the LRO parameter in terms of site occupation probabilities in the group-III sublattice^[17]. This sublattice is divided into two sublattices, α and β , which are occupied respectively by In and Ga in the perfectly

ordered [111] monolayer superlattice. Four site occupation probabilities, p_K^σ , give the fraction of sites in sublattice $\sigma = \alpha$ or β which are occupied by species $K = \text{In}$ or Ga respectively. In terms of these, the alloy composition is $x = (p_{\text{In}}^\alpha + p_{\text{In}}^\beta)/2 = 1 - (p_{\text{Ga}}^\beta + p_{\text{Ga}}^\alpha)/2$, and the LRO parameter is defined as $S = p_{\text{In}}^\alpha - p_{\text{In}}^\beta = p_{\text{Ga}}^\beta - p_{\text{Ga}}^\alpha$. The fully ordered structure corresponds to $x = 0.5$ and $S = 1$ while, for partially ordered configurations, $0 < S < 1$.

Alloys are treated in the small crystal approximation, using a 64-site cubic basic cluster, which contains eight conventional cubic cells of the diamond lattice^[9]. Partially ordered $\text{In}_x\text{Ga}_{1-x}\text{P}$ alloys are simulated through small crystal configurations numerically generated according to the occupation probabilities of the 32 sites of the group-III sublattice: $p_{\text{In}}^\alpha = (2x + S)/2 = 1 - p_{\text{Ga}}^\alpha$, $p_{\text{In}}^\beta = (2 - S)/2 = 1 - p_{\text{Ga}}^\beta$. For the present study, $x = 0.5$, and 400 structures are generated for each value of S in the range $[0, 1]$.

The binary constituents of $\text{In}_x\text{Ga}_{1-x}\text{P}$ present a bond-length mismatch of 7.6%, which results in a strained alloy. The equilibrium atomic positions for each small crystal in the ensemble of configurations was determined^[17] assuming the elastic energies are described by a Keating-type valence force field (VFF) model^[18,19]. The elastic energy was minimized using a molecular-dynamics algorithm^[20], allowing for full unconstrained relaxation of each configuration. Results from the equilibrium configurations are summarized in Fig 2. There, the average nearest-neighbor distances along the [111] ordering direction (O) and along the lateral directions (L) are plotted versus S^2 for Ga-P and In-P bonds. Of course the notation O and L is to be taken as a general indication of the bonds orientation, since in equilibrium the alloy bonds are not strictly parallel to any special direction. Average values for the 4 types of bonds show an excellent quadratic fit for the dependence with the order parameter. In particular, the O - L bond shift may be written as

$$\Delta b(S) = \Delta b_{\text{max}} S^2, \quad (3)$$

with $\Delta b_{\text{max}} = -0.050 \text{ \AA}$ for Ga-P bonds and 0.057 \AA for In-P bonds. Bond lengths for the ordered ($S = 1$) system are in agreement with previous calculations^[19]. O-bonds are very close to the ideal unstrained length value for each bond type, while L-bonds are shifted by Δb_{max} with respect to those. As S decreases from 1 to 0, average O and L bond lengths merge into values which depend only on the species: 2.512 \AA for In-P and 2.383 \AA for Ga-P.

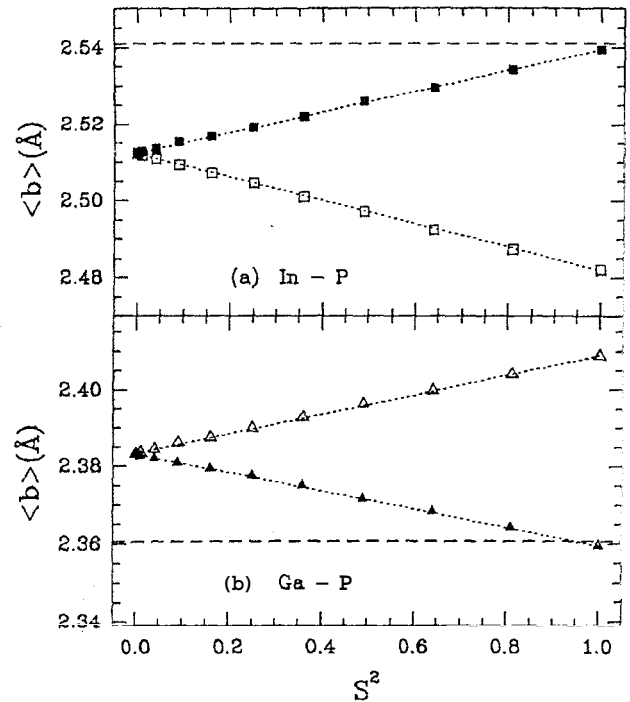


Figure 2: Average calculated lengths of O-bonds (solid symbols) and L-bonds (open symbols) for (a) In-P, and (b) Ga-P bonds, versus the order parameter squared. Statistical error bars are at most equal to symbol size. The corresponding unstrained bond length is given by an horizontal dashed line. Dotted lines indicate the quadratic dependence of average bond lengths with S .

The electronic structure of each small crystal is obtained in the tight-binding approximation^[11] by directly solving for the Hamiltonian spectrum^[17]. Distortions due to stress are incorporated locally in each near-neighbor matrix element through a $(b_0/b_{ij})^2$ scaling^[21], where b_{ij} is the calculated equilibrium distance between atomic sites i and j and b_0 is the unstrained value of the corresponding bond. Fig 3 gives the ensemble average values for the main energy-gap as a function of the order parameter S . As expected, E_g is a decreasing function of S , but, contrary to the structural parameters plotted in Fig 2, a quadratic dependence alone does not describe the calculated trend accurately. Symmetry implies that $E_g(S) = E_g(-S)$, therefore polynomial corrections are restricted to even powers of S . Addition of a small quartic term yields a satisfactory fit, indicated by the dotted line in Fig 2. It corresponds to the form $E_g(S) = E_g(0) - \Delta E_g(S)$, where

$$\Delta E_g(S) = (0.13 S^2 - 0.03 S^4) \text{ eV} \quad (4)$$

is the gap reduction of ordered samples *with respect to the random alloy*.

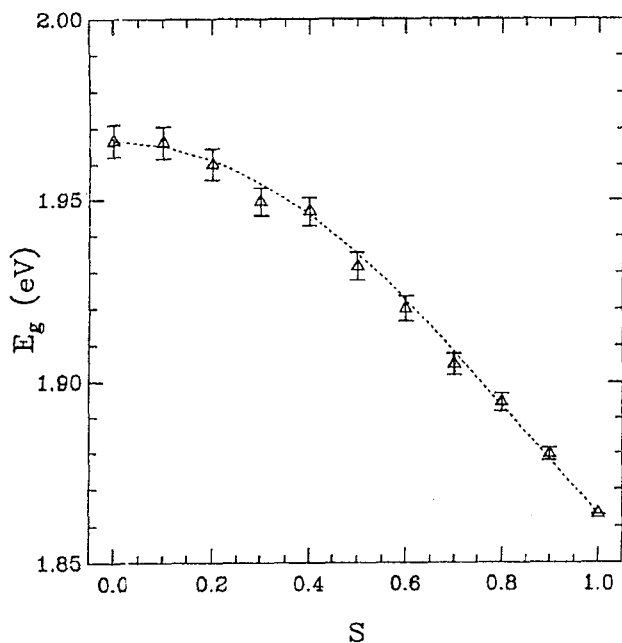


Figure 3: Calculated low temperature energy-gap of $\text{In}_{0.5}\text{Ga}_{0.5}\text{P}$ versus order parameter. Each data point gives the *ensemble* average over 400 64-sites small crystal structures. Statistical error bars are indicated. The dotted line is a fourth-order polynomial fit, described in the text.

All measured gap values given in Ref. [5] for ordered samples fall within the range of our calculation. Assuming our calculated $E_g(S)$ dependence, those would correspond to S between 0.5 and 0.9. The order parameter values estimated there are considerably smaller due to the presumed linear dependence of E_g with S . The lowest value for E_g reported in the literature is 1.868 eV (at $T=4$ K) for a sample grown by atomic layer epitaxy^[15]. From our calculation, this sample would essentially correspond to $S \sim 1$.

The dependence of the gap with S obtained here explains the apparent contradiction described in Ref. [16] of samples with almost "normal" band gaps but still showing order in X-ray diffraction patterns. From Fig 2 we note that for $S < 0.4$ the gap reduction effect is almost negligible (less than 1%), while values of $S \sim 0.4$ would still show superlattice diffraction spots in X-ray experiments.

Our results indicate that local structural measurements provide essential information to establish the degree of ordering in $\text{In}_x\text{Ga}_{1-x}\text{P}$ alloys. Electron diffraction^[4] and X-ray diffraction^[16] experiments show great quantitative uncertainties, while photoluminescence spectra, from which E_g is usually obtained, present a strong and anomalous temperature dependence^[16]. Therefore diffraction spots intensities and band-gap values alone can not give accurate estimates for the LRO parameter. On the other hand, the simple quadratic dependence of the O - L bond shifts with S obtained here may be used as a reliable measure

for the degree of ordering of these alloys. Of course O - L bond shift measurements are also subject to uncertainties, so that trying to infer the absolute value of the order parameter from these experiments is subject to such inaccuracies, and must also be based on a precise knowledge of Δb_{max} . We estimate our value of Δb_{max} is reliable within 0.005 to 0.01 Å, which is comparable to EXAFS experimental accuracy.

Previous studies have mainly dealt with the composition dependence of elastic and electronic properties of semiconductor random alloys. Near-neighbor distances are usually found to follow a linear dependence with x [22,23]. Band gaps, however, show distinct "bowing" effects, and both linear and quadratic terms in x are present in fits to $E_g(x)$ [2]. In the case of order, the simplest functional dependence of physical quantities on *any order parameter* S for which the system has $S \rightarrow -S$ symmetry is quadratic: no linear terms are allowed. For the particular system considered here, this is an excellent approximation for average near-neighbor distances, while gap properties require higher order corrections. The situation is quite analogous to the composition dependence of these quantities, only that expansions are performed in powers of x in one case and in powers of S^2 in the other.

IV. Conclusions

The small crystal formalism presented here is of general application to disordered or partially ordered alloys, and gives direct information about the dependence of different alloy properties on statistical parameters related to composition, long or short range order. Specific properties focused here, namely the change in nature of the optical gap in $\text{Al}_x\text{Ga}_{1-x}\text{As}$, equilibrium bond lengths and order-induced gap reduction effects in $\text{In}_x\text{Ga}_{1-x}\text{P}$ alloys, illustrate the flexibility of this scheme. Previous applications of this method to semiconductor systems include the formation energy of ordered compounds^[7], and pressure effects in $\text{Al}_x\text{Ga}_{1-x}\text{As}$ [9,24]. It is interesting to note that the small crystal approach was originally developed for the study of many-body effects in exactly soluble models^[10]. We have shown that it may be extended to couple statistical mechanics concepts and simulation techniques to standard solid-state methods in a variety of problems involving bulk materials. Future extensions include the study of heterostructures and doping in semiconductor materials.

Acknowledgments

Work partially supported by Ministério de Ciência e Tecnologia, Conselho Nacional de Desenvolvimento Científico e Tecnológico and Fundação de Amparo à Pesquisa do Estado do Rio de Janeiro.

References

1. T. F. Kuech, D. J. Woford, R. Potenski, J. A. Bradley, K. H. Kelleher, D. Yan, J. P. Farrell, P. M. S. Lesser, and F. H. Pollak, *Appl. Phys. Lett.* **51**, 505 (1987).
2. A.-B. Chen and A. Sher, *Piys. Rev. B* **23**, 53G0 (1981).
3. A. Gomyo, K. Kobayashi, S. Kawata, I. Hino, T. Suzuki, and T. Yuasa, *J. Cryst. Growth* **77**, 367 (1986); R. Gomyo, T. Suzuki, K. Kobayashi, S. Kawata, I. Hino, and T. Yuasa, *Appl. Phys. Lett.* **50**, 673 (1987).
4. A. Gomyo, T. Suzuki, and S. Iijima, *Piys. Rev. Lett.* **60**, 2645 (1988).
5. T. Kanata, M. Nishimoto, T. Nakayama, and T. Nishino, *Piys. Rev. B* **45**, 6637 (1992). The order parameter δ in this reference differs from S defined here by a factor of 2.
6. S. R. Kurtz, J. M. Olson, and A. Kibbler, *Appl. Phys. Lett.* **57**, 1922 (1990).
7. B. Koiller, M. A. Davidovici, and L. M. Falicov, *Piys. Rev. B* **41**, 3670 (1990); **42**, 3194(E) (1990).
8. B. Koiller, R. Osório, and L. M. Falicov, *Piys. Rev. B* **43**, 4170 (1991).
9. R. B. Capaz, J. P. von der Weid, and R. Koiller, *Appl. Phys. Lett.* **60**, 704 (1992).
10. L. M. Falicov, in *Recent Progress in Many-Body Theories*, edited by E. Pajane and R. F. Bishop (Plenum, New York, 1988), Vol. 1, p.275.
11. P. Vogl, H. P. Hjalmarson, and J. D. Dow, *J. Piys. Chem. Solids* **44**, 365 (1983).
12. D. Stauffer, *Introduction to Percolation Theory* (Taylor and Francis, London, 1985).
13. K. Binder and D. W. Heermann, *Monte Carlo Simulation in Statistical Physics* (Springer-Verlag, Berlin, 1988).
14. T. Nishino, Y. Inoue, Y. Hamakawa, M. Kondow, and S. Minagawa, *Appl. Phys. Lett.* **53**, 583 (1988); M. Kondow, H. Kakibayashi, S. Minagawa, Y. Inoue, T. Nishino, and Y. Hamakawa, *Appl. Phys. Lett.* **53**, 2053 (1988).
15. B. T. McDermott, K. G. Reid, N. A. El-Masry, S. M. Bedair, W. M. Duncan, X. Yin, and F. H. Pollak, *Appl. Phys. Lett.* **56**, 1172 (1990).
16. S. R. Kurtz, J. M. Osloii, and A. Kibbler, *Appl. Phys. Lett.* **54**, 718 (1989).
17. R. B. Capaz and B. Koiller, *Piys. Rev. B* **47**, 4044 (1993).
18. P. N. Keating, *Piys. Rev.* **145**, 637 (1966).
19. T. Kurimoto and N. Hamada, *Piys. Rev. B* **40**, 3889 (1989).
20. B. Koiller and M. O. Robbins, *Piys. Rev. B* **40**, 12554 (1989).
21. W. H. Harrison, *Electronic Structure and the Properties of Solids* (W. H. Freeman, San Francisco, 1980).
22. J. B. Boyce and J. C. Mikkelsen, Jr, in *Ternary and Multiternary Compounds*, Proceedings of the Seventh International Conference, edited by S. K. Deb and A. Zunger (Materials Research Society, Pittsburgh, 1987), p. 359.
23. J. C. Mikkelsen, Jr and J. B. Boyce, *Piys. Rev. Lett.* **49**, 1412 (1982).
24. R. B. Capaz, G. C. de Araújo, B. Koiller, and J. P. von der Weid, to be published.